Pilot-Symbol-Aided 16PSK and 16QAM for Digital Land Mobile Radio Systems

Wireless Personal Communications

Key words:

Fading Compensation, Pilot-Symbols Aided, PSK, QAM, Rayleigh Fading

H. K. LAU   S. W. CHEUNG*
hklau@hkueee.hku.hk   swcheung@hkueee.hku.hk

Department of Electrical and Electronic Engineering
The University of Hong Kong
Pokfulam Road
HONG KONG
Phone: (852) 2859-2425
Fax: (852) 2559-8738

* Please send all correspondence to Dr. S. W. CHEUNG

ABSTRACT

The paper proposes a novel pilot-symbol-aided (PSA) technique for fading compensation of digital signals in the mobile environments. In a PSA system, the data sequence at the transmitter is divided into frames of data. A pilot symbol from a known pseudoradom-symbol sequence is inserted periodically into a frame of data symbol for transmission. In a conventional PSA-receiver, these pilot symbols are extracted from the received signal and used to estimate the effects of signal distortion introduced in the fading channel. The resultant estimates are then used to correct the distortion effects in the received data frames. In the paper, a novel estimation technique that uses the data symbols as well as the pilot symbols is proposed. The technique has the major advantages of simple implementation and short storage-delay time. Results are presented in a series of computer-simulation tests. These assess the effectiveness of the estimation technique on the BER performances of a 16-ary phase-shift keyed (16PSK) and a 16-ary quadrature-amplitude modulated (16QAM) signals in the frequency-selective and frequency-nonselective Rayleigh fading channels. The channels are corrupted by co-channel interference or additive white Gaussian noise. Results of differential-detected 16PSK and star-16QAM signals are also presented for comparison. It has been shown that, the use of PSA technique can significantly improve the bit-error-rate performances of the systems, relative to those using differential detection.

I. INTRODUCTION

In the design of digital modems for mobile radio communications systems, the signal distortion introduced in the fading channels imposes the restrictions on the modulation techniuqes which can be used. In order to minimize the signal distortion which results from fading, a near-constant envelope signal is normally used. Thus the Gaussian-minimum-shift keyed (GMSK) and quaternary-phase-shift keyed (QPSK) signals with a theoretical spectral efficiency of only two bit/s/Hz are most often used over mobile links. However, with the ever-increasing demands for the RF bandwidth allocations, there will be a severe shortage of RF spectrum for digital land mobile radio systems and the signals with better spectral efficiencies are expected to be used in future. Among these spectrally efficient signals, the 16-ary phase-shift keyed (16PSK) and 16-ary quadrature-amplitude-modulated (16QAM) signals with a theoretical spectral efficiency of four bit/s/Hz are promising candidates because of their relative simplicity of implementation and good bit-error-rate (BER) performance through linear channels [1-2]. Recently, the pilot-symbol-aided (PSA) transmission techniques have been proposed to compensate the signal distortion when this type of signals is transmitted in the fading channels [3-9]. In a PSA system, the transmitted data-symbol sequence is divided into frames of data symbols. A pilot symbol from a known pseudorandom-symbol sequence is then inserted into each of these frames for transmission. The receiver is assumed to have prior knowledge of the pilot-symbol sequence and so is able to extract the pilot symbols from the received signal and hence to estimate the signal distortion introduced in the fading channel. The resultant estimates are then used to correct the fading effects in the data symbols. Different algorithms have been proposed to estimate the fading effects using the received pilot symbols. In these studies, the fading estimation processes make use of only the pilot symbols but ignore the fading distortion information in the data symbols [3-7]. Several simple estimation techniques that make use of the data symbols as well as the pilot symbols to enhance the accuracy of the estimation process have been proposed by the authors [8-9]. Studies have shown that, in the frequency non-selective fading channels, substantial improvements on BER performances of the signals can be

achieved by using both the pilot and data symbols, instead of only the pilot symbols, for fading estimation.

This paper studies a first-order estimation technique [8] to be used in the frequency-selective and frequency-nonselective Rayleigh fading channels that corrupted by co-channel interference (CCI) or additive white Gaussian noise (AWGN). The major advantages of the proposed technique are its simple implementation and the short storage-delay time introduced. Since it requires only two pilot symbols to compensate the fading effects of the data symbols within a frame, the storage-delay time is only one frame long. Results are presented in a series of computer-simulation tests. These assess the effectiveness of the technique on the BER performances of the 16PSK and 16QAM signals. Since the 16PSK and star-16QAM signals can be differentially detected, they can be used for mobile systems [11]. The BER performances of the differential-detected 16PSK (DD-16PSK) and star-16QAM signals are also presented for comparison. It has been shown that, under all the conditions tested, the PSA-16QAM signal has the best BER performances.

The paper is organized as follows. Section II describes the system model used for the study. The proposed fading compensation technique is described in section III. Simulation results and discussions are presented in section IV.

II. SYSTEM MODEL

The baseband equivalent model of the data-transmission system used in the study is shown in Fig. 1. In the transmitter, the encoder maps the binary data $\{u_n\}$ into the data symbols $\{d_{k,i}\}$ according to the 16PSK or 16QAM signal constellations shown in Fig. 2. For every $(L-1)$-data symbols, a pilot symbol from a known pseudoradom-symbol sequence $\{p_{k,0}\}$ is inserted at the beginning of the frame to form an L-symbol frame as shown in Fig. 3. (A pseudoradom sequence of pilot symbols is used to avoid transmitting tones [4].) To minimize the performance degradation due to AWGN, the pilot symbols are chosen to be those symbols with the largest energy levels in the signal constellation [6]. In Fig. 1, at time $t = nT$ seconds, the transmitted (data or pilot) symbol is used to form an impulse $q_n \delta(t - nT)$ which is fed to the premodulation filter with an impulse response $a(t)$. The signal q_n is either a data symbol $d_{k,i}$ or pilot symbol $p_{k,0}$ and is complex-valued, and $\delta(t)$ is the Dirac-delta function. At the output of the premodulation filter, the signal $\sum_n q_n a(t - nT)$ is used to linearly modulate the carrier signal to form the transmit signal.

Each of the transmission paths (transmission paths 1, 2 and 3) in Fig. 1 introduces uncorrelated Rayleigh fading distortion [10] to the corresponding input signal and is modeled as shown in Fig. 4, where the input signal is multiplied by the complex-valued low frequency Gaussian waveform

$$b(t) = b'(t) + jb''(t) \tag{1}$$

to give the corresponding Rayleigh-faded signal. The waveforms $b'(t)$ and $b''(t)$ are two statistically independent real-valued baseband Gaussian waveforms, each with the power spectral density of [1]

$$|B(f)|^2 = \begin{cases} \dfrac{\sigma^2}{\pi\sqrt{f_D{}^2 - f^2}}, & -f_D \le f \le f_D \\ \\ 0, & \text{elsewhere} \end{cases} \tag{2}$$

where $|B(f)|$ is the magnitude of $B(f)$, σ^2 is the average power of the faded carrier, and f_D is the maximum Doppler spread of the faded signal caused by the mobile motion and given by

$$f_D = \frac{v}{\lambda} \tag{3}$$

where v is the velocity of the mobile and λ is the wavelength of the signal carrier. To generate $b'(t)$ and $b''(t)$, two statistically independent stationary real-valued white Gaussian noise waveforms are fed separately into two identical lowpass filters with the same transfer function given by (2). In each of the transmission paths in Fig. 1, the input signal is multiplied by an individual (uncorrelated) complex-valued signal $b(t)$ to give the corresponding Rayleigh-faded signal. The combination of the desired (main-path) signal and the delayed signal accounts for frequency-selective fading of the channel [10]. Stationary white Gaussian noise is assumed to be added at the input of the receiver. Thus at the input of the receiver (Fig. 1), the signal composes of the desired signal (from transmission path 1), the delayed signal (from transmission path 2), the CCI signal (from transmission path 3) and AWGN. The received signal is filtered by a postdemodulation filter which is taken to have the same impulse response $a(t)$ as the premodulation filter at the transmitter, so that the signal at the output of the postdemodulation filter is given by

$$r(t) = \sum_n q_n a(t - nT) y(t) * a(t) + w(t) \tag{4}$$

where $*$ denotes the convolution process, $y(t)$ represents the combined distortion effects introduced into the desired signal by the three transmission paths and $w(t)$ is the filtered noise waveform. Assume the Doppler shift due to the mobile motion is small compared to the symbol rate and so the intersymbol interference (ISI) caused by the filtering process can be neglected. The baseband signal $r(t)$ is sampled in synchronism at the time instants $\{nT\}$. Also assume $a(t) * a(t) = 1$ at time $t = 0$, so the signal at time $t = nT$ is given by

$$r_n = q_n y_n + w_n \tag{5}$$

where $y_n = y(nT)$ and $w_n = w(nT)$. Since the transmitted pilot symbols are known at the receiver, in the absence of AWGN, the effects of distortion y_n on the pilot symbol is computed as

$$y_n = \frac{r_n}{q_n} \tag{6a}$$

However, in the presence of AWGN, only an estimate of y_n can be obtained as

$$\hat{y}_n = \frac{r_n}{q_n} \tag{6b}$$

which is used to estimate the distortion effects on the received data symbols. The estimates are used to correct the data symbols which are then fed to the detector and decoder to produce the binary data $\{\hat{u}_n\}$ at the output. The proposed estimation technique is described in the following section.

III. MULTIPATH FADING COMPENSATION

The frame structure of the transmitted symbol sequence is shown in Fig. 3. The signal at the i-th position of the k-th received frame can be written as

$$r_{k,i} = q_{k,i} y_{k,i} + w_{k,i} \tag{7a}$$

where $q_{k,i}$ is either a transmitted pilot symbol or a transmitted data symbol, $y_{k,i}$ is the distortion effects (combines the effects of the fading distortion in transmission path 1, the delayed signal from transmission path 2 and the CCI signal from transmission path 3) on the i-th symbol of the k-th frame, and $w_{k,i}$ is the noise at the i-th symbol of the k-th frame.

For $i = 0$, the signal is

$$r_{k,0} = p_{k,0} y_{k,0} + w_{k,0} \tag{7b}$$

where $p_{k,0}$ is the pilot symbol in the k-th frame. For $i = 1, 2, ..., L$-1, the signal is

$$r_{k,i} = d_{k,i} y_{k,i} + w_{k,i} \tag{7c}$$

where $d_{k,i}$ is a data symbol at the i-th symbol of the k-th frame. The proposed compensation process works with the frame lengths of 4, 8, ..., or 2^m (where m is a positive integer) and consists of two compensation stages. The first stage works on the data symbols in the even-number positions (i.e., $i = 2, 4, ..., L$-2), while the second stage works on the data symbols in the odd-number positions (i.e., $i = 1, 3, ..., L$-1) of a frame.

Compensation for Data Symbols in Even-Number Positions

The combined distortion effects, $\hat{y}_{k,0}$ and $\hat{y}_{k+1,0}$, on the pilot symbols, $p_{k,0}$ and $p_{k+1,0}$, in the k-th and $(k+1)$-th frames, respectively, due to the three transmission paths are estimated as

$$\hat{y}_{k,0} = \frac{r_{k,0}}{p_{k,0}} \tag{8a}$$

$$\hat{y}_{k+1,0} = \frac{r_{k+1,0}}{p_{k+1,0}} \tag{8b}$$

The estimate of the distortion effects on the data symbol, $d_{k,L/2}$, is computed as

$$\hat{y}_{k,L/2} = \frac{\hat{y}_{k,0} + \hat{y}_{k+1,0}}{2} \tag{9a}$$

This signal is then used to correct the distortion effects in $r_{k,L/2}$ to give an estimate of the data symbol

$$\hat{r}_{k,L/2} = \frac{r_{k,L/2}}{\hat{y}_{k,L/2}} \tag{9b}$$

This corrected data symbol is threshold detected to produce the detected data symbol $\hat{d}_{k,L/2}$ (where $\hat{d}_{k,L/2}$ is a possible signal vector on the constellation). If $L = 4$, the compensation process for the data symbols in the even-number positions is completed and the compensation process for the data symbols in the odd-number positions begins.

If $L = 8$, the compensation process for the data symbols in the even-number positions continues as follows. The detected data symbol $\hat{d}_{k,L/2}$ is used to estimate $y_{k,L/2}$ as $r_{k,L/2}/\hat{d}_{k,L/2}$ which is then used to obtain the estimates of $y_{k,L/4}$ and $y_{k,3L/4}$ as

$$\tilde{y}_{k,L/4} = \frac{1}{2}\left(\hat{y}_{k,0} + \frac{r_{k,L/2}}{\hat{d}_{k,L/2}} \right) \tag{10a}$$

$$\tilde{y}_{k,3L/4} = \frac{1}{2}\left(\frac{r_{k,L/2}}{\hat{d}_{k,L/2}} + \hat{y}_{k+1,0} \right) \tag{10b}$$

respectively. These signals $\tilde{y}_{k,L/4}$ and $\tilde{y}_{k,3L/4}$ are used to correct $r_{k,L/4}$ and $r_{k,3L/4}$ to obtain the corrected data symbols

$$\hat{r}_{k,L/4} = \frac{r_{k,L/4}}{\tilde{y}_{k,L/4}} \tag{10c}$$

$$\hat{r}_{k,3L/4} = \frac{r_{k,3L/4}}{\tilde{y}_{k,3L/4}} \tag{10d}$$

which are threshold detected to produce the corresponding data symbols $\hat{d}_{k,L/4}$ and $\hat{d}_{k,3L/4}$.

If $L = 16$, the compensation process continues further. The detected data symbols, $\hat{d}_{k,L/4}$ and $\hat{d}_{k,3L/4}$, are used to obtain the estimates of $y_{k,L/4}$ and $y_{k,3L/4}$ as $r_{k,L/4}\big/\hat{d}_{k,L/4}$ and $r_{k,3L/4}\big/\hat{d}_{k,3L/4}$, respectively. Then together with $\hat{y}_{k,0}$ and $\hat{y}_{k+1,0}$, the estimates of the effects on the rest of the symbols within the frame are obtained according to

$$\tilde{y}_{k,L/8} = \frac{1}{2}\left(\hat{y}_{k,0} + \frac{r_{k,L/4}}{\hat{d}_{k,L/4}} \right) \tag{11a}$$

$$\tilde{y}_{k,7L/8} = \frac{1}{2}\left(\frac{r_{k,3L/4}}{\hat{d}_{k,3L/4}} + \hat{y}_{k+1,0} \right) \tag{11b}$$

$$\tilde{y}_{k,jL/8} = \frac{1}{2}\left(\frac{r_{k,(j-1)L/8}}{\hat{d}_{k,(j-1)L/8}} + \frac{r_{k,(j+1)L/8}}{\hat{d}_{k,(j+1)L/8}} \right) \quad \text{for } j = 3,\, 5 \tag{11c}$$

These estimates are used to correct the corresponding received data symbols. Here again, the corrected data symbols are then fed to the threshold detector to produce the detected data symbols. A set of equations similar to (11) can be derived for $L = 32, 64, ..., 2^m$ (where m is a positive integer). The compensation process continues until all the data symbols in the even-number positions are done. The compensation process for the data symbols in the odd-number positions then begins.

Compensation for Data Symbols in Odd-Number Positions

The compensation process for the data symbols in the odd-number positions is straightforward. The distortion effects on the data symbols are estimated as

$$\tilde{y}_{k,1} = \frac{1}{2}\left(\hat{y}_{k,0} + \frac{r_{k,2}}{\hat{d}_{k,2}} \right) \tag{12a}$$

$$\tilde{y}_{k,L-1} = \frac{1}{2}\left(\frac{r_{k,L-2}}{\hat{d}_{k,L-2}} + \hat{y}_{k+1,0}\right) \tag{12b}$$

$$\tilde{y}_{k,j} = \frac{1}{2}\left(\frac{r_{k,j-1}}{\hat{d}_{k,j-1}} + \frac{r_{k,j+1}}{\hat{d}_{k,j+1}}\right) \text{ for } j = 3, 5, ..., L\text{-}3 \tag{12c}$$

The corrected data symbols are then obtained as

$$\hat{r}_{k,i} = \frac{r_{k,i}}{\tilde{y}_{k,i}} \qquad \text{for } i = 1, 3, ..., L\text{-}1 \tag{13}$$

which are fed to the threshold detector to produce the detected data symbols. Of course, at the end of the compensation process, all the detected data symbols are fed to the encoder to produce the binary data $\{\hat{u}_n\}$.

The whole compensation process repeats for all the received frames. It should be noted that the major advantages of the proposed estimation technique are simple implementation and the short storage-delay time introduced by the fading compensation process. It requires only two pilot symbols to compensate all the data symbols within a frame, so the storage-delay time is only one frame long.

Signal Energy Considerations

Since the pilot symbols are known to the receiver, they carry no data information, but require a certain amount of power for transmission. Thus for a system with a fixed transmission power, a portion of the power has to be assigned for transmitting the pilot symbols. The net average data-symbol energy is therefore reduced. If the same transmit data-symbol energy as that without transmitting the pilot symbols is to be maintained, the average energy per data symbol has to be increased by

$$\Delta E_s = 10 \log\left[\left(\frac{L}{L-1}\right)\left(\frac{|P_d|\cdot\frac{L-1}{L} + |P_p|\cdot\frac{1}{L}}{|P_d|}\right)\right] \text{dB}$$

$$= 10 \log \left[\left(\frac{|P_p|}{|P_d|} \right) \left(\frac{1}{L-1} \right) + 1 \right] \text{ dB} \tag{14a}$$

where L is the frame length, $|P_p|$ and $|P_d|$ are the average energies required to transmit a pilot symbol and a data symbol, respectively.

For 16PSK signal, all the signal vectors have the same energy level, and (14a) reduces to

$$\Delta E_s = 10 \log \left(\frac{L}{L-1} \right) \text{ dB} \tag{14b}$$

For 16QAM signal, since the pilot symbols are selected from those signal vectors with the largest signal levels in the constellation, $|P_p| : |P_d| = 9 : 5$ and (14a) becomes

$$\Delta E_s = 10 \log \left[\frac{9}{5} \left(\frac{1}{L-1} \right) + 1 \right] \text{ dB}$$

$$= 10 \log \left[\frac{5L+4}{5(L-1)} \right] \text{ dB} \tag{14c}$$

The theoretical BER performances of coherent 16PSK and 16QAM signals in a Gaussian channel are given by [12]

$$P_{b,16PSK} \approx \frac{1}{4} \text{erfc} \left[\sqrt{\frac{4E_b}{N_0}} \sin \left(\frac{\pi}{16} \right) \right] \tag{15a}$$

$$P_{b,16QAM} \approx \frac{3}{8} \text{erfc} \left(\sqrt{\frac{6E_b}{15N_0}} \right) \times \left[1 - \frac{3}{8} \text{erfc} \left(\sqrt{\frac{6E_b}{15N_0}} \right) \right] \tag{15b}$$

where E_b is the average energy required to transmit a bit, and N_0 is the single-sided noise power spectral density of the AWGN. Taking into account the loss of energy due to transmitting the pilot symbols, the BER performances of these two signals over a Gaussian channel, with different values of frame length L, become

$$P_{b,16PSK} \approx \frac{1}{4} \, \mathrm{erfc} \left[\sqrt{4 \left(\frac{E_b}{N_0} - \Delta E_s \right)} \sin \left(\frac{\pi}{16} \right) \right] \tag{16a}$$

$$P_{b,16QAM} \approx \frac{3}{8} \, \mathrm{erfc} \left[\sqrt{\frac{6}{15} \left(\frac{E_b}{N_0} - \Delta E_s \right)} \right] \times \left\{ 1 - \frac{3}{8} \, \mathrm{erfc} \left[\sqrt{\frac{6}{15} \left(\frac{E_b}{N_0} - \Delta E_s \right)} \right] \right\} \tag{16b}$$

where ΔE_s is given by (14b) and (14c) respectively. The BER performances of the 16PSK and 16QAM signals, with the insertion of pilot symbols and different frame lengths, are shown in Fig. 5. No compensation technique is used in these systems. It can be seen that, as the frame length increases, the performance degradation due to transmitting the pilot symbols reduced. When the frame length of $L = 8$, the performance degradations of 16PSK and 16QAM signals caused by transmitting the pilot symbols are about 0.58 dB (using (14b)) and 0.99 dB (using (14c)), respectively.

Bandwidth Considerations

In addition to signal energy, a certain amount of bandwidth is also required to transmit the pilot symbols. If the same system throughput as that without transmitting the pilot symbols is to be maintained, the resultant symbol rate needs to be increased by a factor of $L/(L-1)$. For a frame length of $L = 8$, there is a 12.5 % loss in the throughput. Obviously, a signal with a shorter frame length requires more extra bandwidth and extra energy for transmitting the pilot symbols. However, a shorter frame length provides a more accurate result on fading estimation [7] and so a compromise has to be reached.

IV.   RESULTS AND DISCUSSIONS

A series of computer-simulation tests has been carried out to study the BER performances of the pilot-symbol-aided-16PSK (PSA-16PSK) and pilot-symbol-aided-16QAM (PSA-16QAM) signals in the mobile radio channels that corrupted by CCI or AWGN. A frame length of $L = 8$, a bit rate of 32 kbit/s and a traveling velocity of 48 km/hr (leading to a normalized Doppler spread of 0.005 at a carrier frequency of 900 MHz) are used throughout the tests. For the purpose of comparison, the results on the BER performances of the differential-detected 16PSK (DD-16PSK) and star-16QAM signals are also presented.

Basic Assumptions

In the study, the signal-to-noise ratio is defined as

$$\text{SNR} = 10\log\left(\frac{E_b}{N_0}\right) \tag{17}$$

where E_b is the average transmitted bit energy (after taking into account the power loss due to transmitting the pilot symbols) and N_0 is the single-sided power spectral density of the AWGN. The signal-to-CCI power ratio is defined as

$$\text{SIR} = 10\log\left(\frac{S}{I}\right) \tag{18}$$

where S and I are the power of the main-path signal and the CCI signal, respectively. The main-path-to-delayed-path power ratio is defined as

$$\text{SDR} = 10\log\left(\frac{S}{D}\right) \tag{19}$$

where D is the signal power of the delayed-path and, of course, if $\text{SDR} = \infty$ dB, the channel becomes frequency-nonselective. The normalized delay between the signals from the main-path and the delayed-path is defined as

$$\frac{\tau}{T} \tag{20}$$

where τ is the time-delay between the main-path and the delayed-path and T is the symbol duration.

Results and Discussions

The simulation results on the BER performances of the signals against SNR, in the frequency-nonselective fading environments ($\text{SDR} = \infty\,\text{dB}$) and in the absence of CCI ($\text{SIR} = \infty\,\text{dB}$) are shown in Fig. 6. The BER performances of the DD-16PSK and star-16QAM signals under the same conditions are also shown for comparison. The star-16QAM signal has the signal constellation shown in Fig. 2c. It can be seen in Fig. 6 that both signals using the PSA technique perform substantially better than the other two signals using differential detection. In addition, the PSA-16QAM signal has the best BER performances. With $\text{SNR} = 50\,\text{dB}$, the PSA-16QAM signal achieves a BER of about 2.2×10^{-5}. While the DD-16PSK and star-16QAM signals have the BERs of only about 1.8×10^{-3} and 5.2×10^{-4}, respectively. Thus the PSA-16QAM signal outperforms the DD-16PSK and star-16QAM signals by the factors of 81.8 and 23.6, respectively.

In the absence of noise ($\text{SNR} = \infty\,\text{dB}$), the BER performances of the signals against SIR in the frequency-nonselective fading environments ($\text{SDR} = \infty\,\text{dB}$) are shown in Fig. 7, which indicates that both signals employing the PSA technique have better tolerances to CCI. Here the PSA-16QAM signal also achieves the best performances. With $\text{SIR} = 50\,\text{dB}$, the BER of the PSA-16PSK and PSA-16QAM signals achieve the BERs of about 9.1×10^{-5} and 4.3×10^{-5}, respectively. While the DD-16PSK and star-16QAM signals only have the BERs of about 1.7×10^{-3} and 5.8×10^{-4}, respectively. Thus the PSA-16QAM signal outperforms the DD-16PSK and star-16QAM signals by the factors of about 39.5 and 13.5, respectively.

In the frequency-selective fading environments ($\text{SDR} \neq \infty\,\text{dB}$), the BER floors ($\text{SNR} = \infty\,\text{dB}$ and $\text{SIR} = \infty\,\text{dB}$) of the signals with the normalized delays $\tau / T = 0.125$ and $\tau / T = 0.5$ are shown in Fig. 8. It can be seen that the BER floors of the PSA-16PSK and

PSA-16QAM signals are substantially lower than those of the DD-16PSK and star-16QAM signals. When the amount of normalized delay is small, the PSA-signals start gaining advantages over the other two signals at a lower value of SDR. TABLE 1 summarizes the minimum SDR required to achieve a BER floor of 1.0×10^{-3} (typical error rate required for voice communications) at the normalized delays of $\tau / T = 0.125$ and $\tau / T = 0.5$. It is shown than the DD-16PSK signal cannot achieve such a BER floor at all the tested SDRs. Here, the PSA-16QAM signal again performs the best among all the signals tested.

TABLE 1. Minimum SDR Required to Achieve a BER Floor of 1.0×10^{-3}

Minimum Required SDR	$\tau / T = 0.125$	$\tau / T = 0.5$
PSA-16QAM	11 dB	29 dB
PSA-16PSK	15 dB	32 dB
Star-16QAM	19 dB	37 dB

When the signal from the delayed-path is 3 dB below that of the desired signal (which indicates a relatively strong main-path component), the BER floors of the PSA-16PSK, PSA-16QAM, DD-16PSK and star-16QAM signals with different values of normalized delay are shown in Fig. 9. It can be seen that the amount of normalized delay has significant effects on the BER floor. The longer the normalized delay, the higher is the BER floor, as is expected. When $\tau / T \geq 0.5$, none of the signals is able to achieve the BER floor lower than 1.0×10^{-1} at SDR = 3 dB. However, the PSA-16QAM signal still performs the best among the signals under tested.

V.   CONCLUSIONS

A novel and simple technique that uses the received data symbols as well as the pilot symbols for fading compensation in the mobile radio channels has been proposed. The major advantages of the technique are simple implementation and the short storage-delay time. Since it requires only two pilot symbols to compensate the fading effects of all the data symbols within a frame, the storage-delay time introduced by the compensation process is only a frame long. The effects of the technique on the BER performances of the 16PSK and 16QAM signals have been studied using computer simulations. The comparisons with those of the DD-16PSK and star-16QAM signals have been made. Results have shown that, under the range of conditions tested, the PSA-16QAM signal has the best performance.

In the frequency-nonselective fading environments and in the absence of CCI, the PSA-16QAM signal achieves a BER of about 2.2×10^{-5} at SNR = 50 dB. However, under the same assumed conditions, the DD-16PSK and star-16QAM signals have the BERs of about 1.8×10^{-3} and 5.2×10^{-4}, respectively. Thus, the PSA-16QAM outperforms the DD-16PSK and star-16QAM signals by the factors of 81.8 and 23.6, respectively. In the absence of noise but presence of CCI with SIR = 50 dB, the BERs of the DD-16PSK and star-16QAM signals are about 1.7×10^{-3} and 5.8×10^{-4}, respectively. While the PSA-16QAM achieves a BER of 4.3×10^{-5}. Here, the PSA-16QAM outperforms the DD-16PSK and star-16QAM signals by the factors of 39.5 and 13.5, respectively.

In the frequency-selective fading environments, the BER floors of the PSA signals are substantially lower than those of the DD-16PSK and star-16QAM signals. When the normalized delay is small, the PSA-signals start gaining advantages at a lower value of SDR. Here, the PSA-16QAM signal again has the best performances.

REFERENCES

[1] K. Feher, *Advanced Digital Communications: Systems and Signal Processing Technqiues*. New Jersey, Prentice-Hall, 1987.

[2] W. T. Webb and L. Hanzo, *Modern Quadrature Amplitude Modulation*. Pentech Press, 1994.

[3] S. Sampei and T. Sunaga, "Rayleigh Fading Compensation Method for 16QAM in Digital Land Mobile Radio Channels," in *Proceedings of IEEE 39th Vehicular Technology Conference,* San Francisco, pp. 640-646, May 1989.

[4] J. K. Cavers, "An Analysis of Pilot Symbol Assisted Modulation for Rayleigh Fading Channels," *IEEE Transactions on Vehicular Technology*, vol. 40, no. 4, pp. 686-693, Nov. 1991.

[5] C. L. Liu and K. Feher, "Pilot-Symbol Aided Coherent *M*-ary PSK in Frequency-Selective Fast Rayleigh Fading Channels," *IEEE Transactions on Communications*, vol. 42, no. 1, pp. 54-62, Jan. 1994.

[6] H. K. Lau and S. W. Cheung, "A Pilot Symbol-Aided Technique Used for Digital Signals in Multipath Environments," in *Proceedings of IEEE International Conference on Communications*, New Orleans, USA, May 1994, pp. 1126-1130.

[7] P. Ho and J. H. Kim, "Pilot Symbol-Assisted Detection of CPM Schemes Operating in Fast Fading Channels," *IEEE Transactions on Communications*, vol. 44, no. 3, pp. 337-347, Mar. 1996.

[8] H. K. Lau and S. W. Cheung, "Multipath fading Compensation Techniques Using Pilot and Data Symbols in Mobile Radio Channels," in *Proceedings of IEEE GLOBECOM Conference*, San Francisco, USA, Nov. 1994, pp. 1009-1013.

[9] H. K. Lau and S. W. Cheung, "A Fade-Compensation Technique for Digital Land Mobile Satellite Systems," accepted, to appear in *International Journal of Satellite Communications*.

[10] Electronic Industries Association Specification IS-54, *Dual-Mode Subscriber Equipment Compatibility Specification*, EIA Project Number 2215, Dec. 1989.

[11] W. T. Webb, "Modulation Methods for PCNs," *IEEE Communications Magazine*, vol. 30, no. 12, pp. 90-95, December 1992.

[12] M. C. Jeruchim, P. Balaban, and K. S. Shanmugan, *Simulation of Communication Systems*, Plenum Press, New York, pp. 706-708.

LIST OF FIGURES
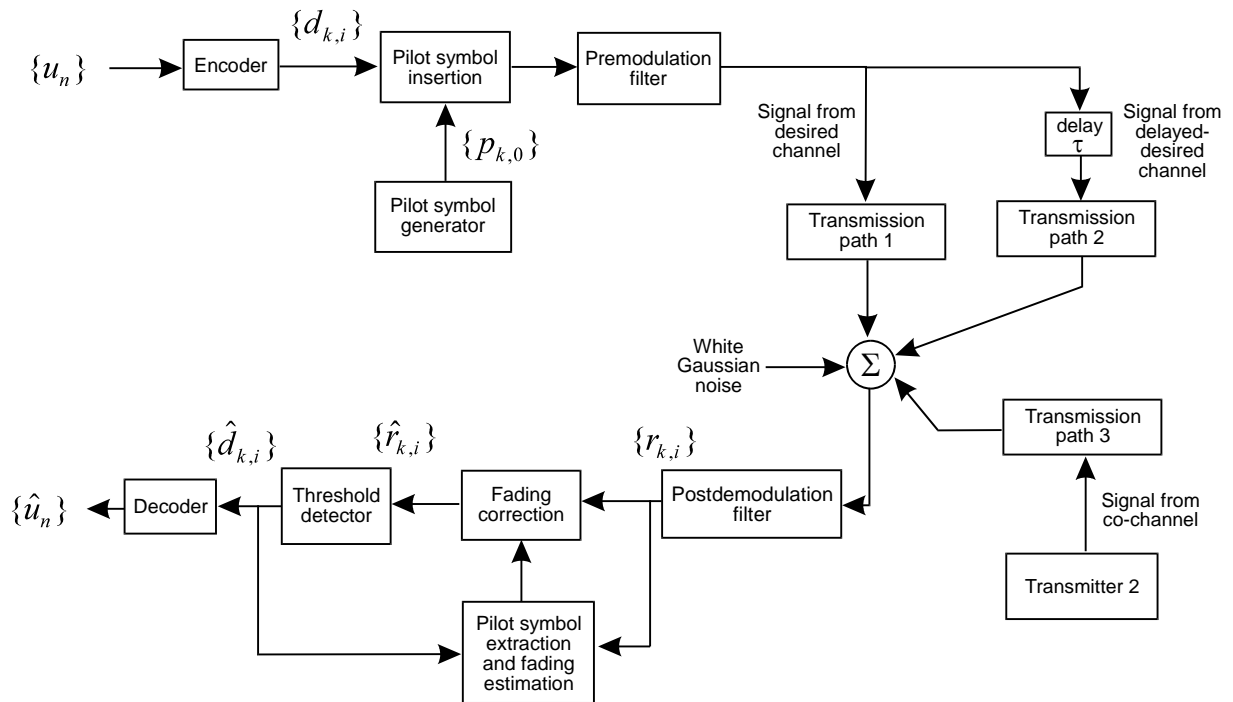
Fig. 1   *Model of System*
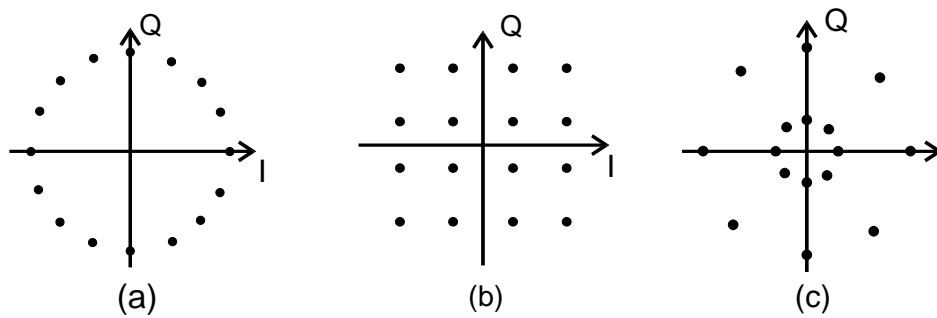

Fig. 2   *Signal Constellations. (a) 16PSK (b) 16QAM (c) Star-16QAM*
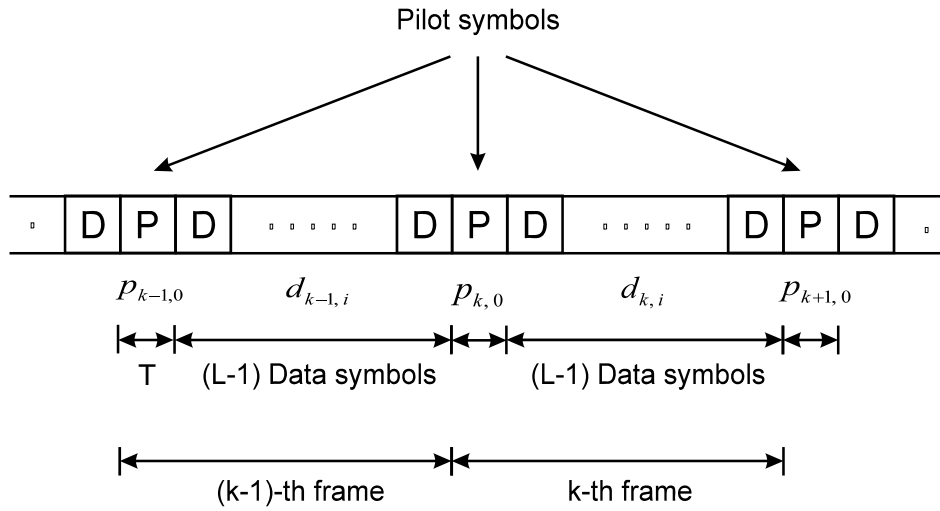
Fig. 3   *Frame Structure of Transmitted Symbol Sequence*
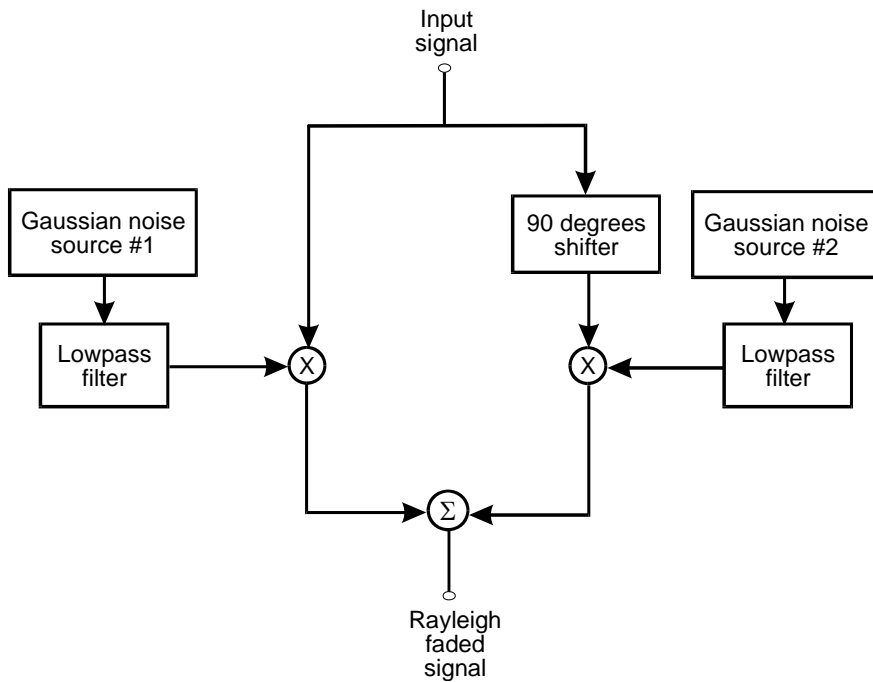

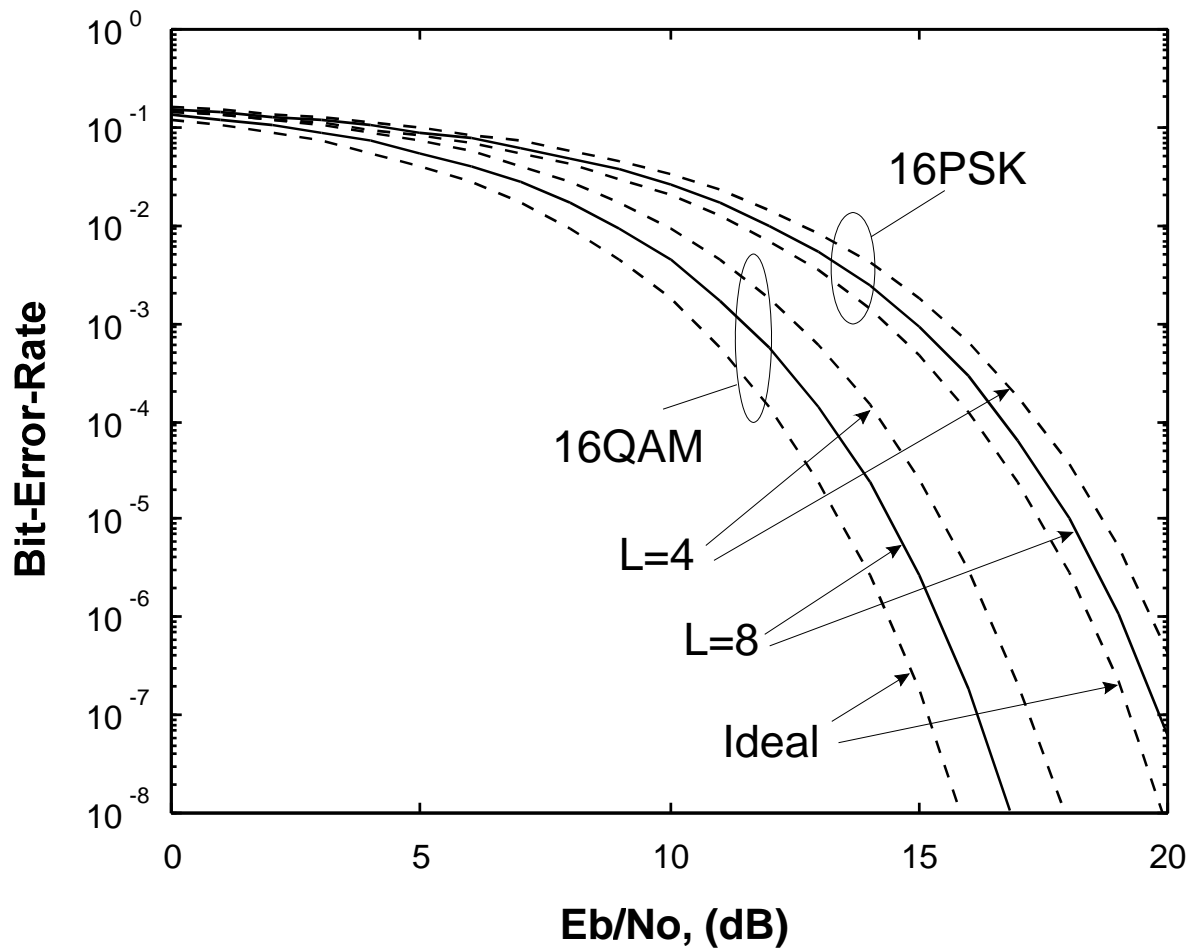**Fig. 4**   *Model of Rayleigh Fading*

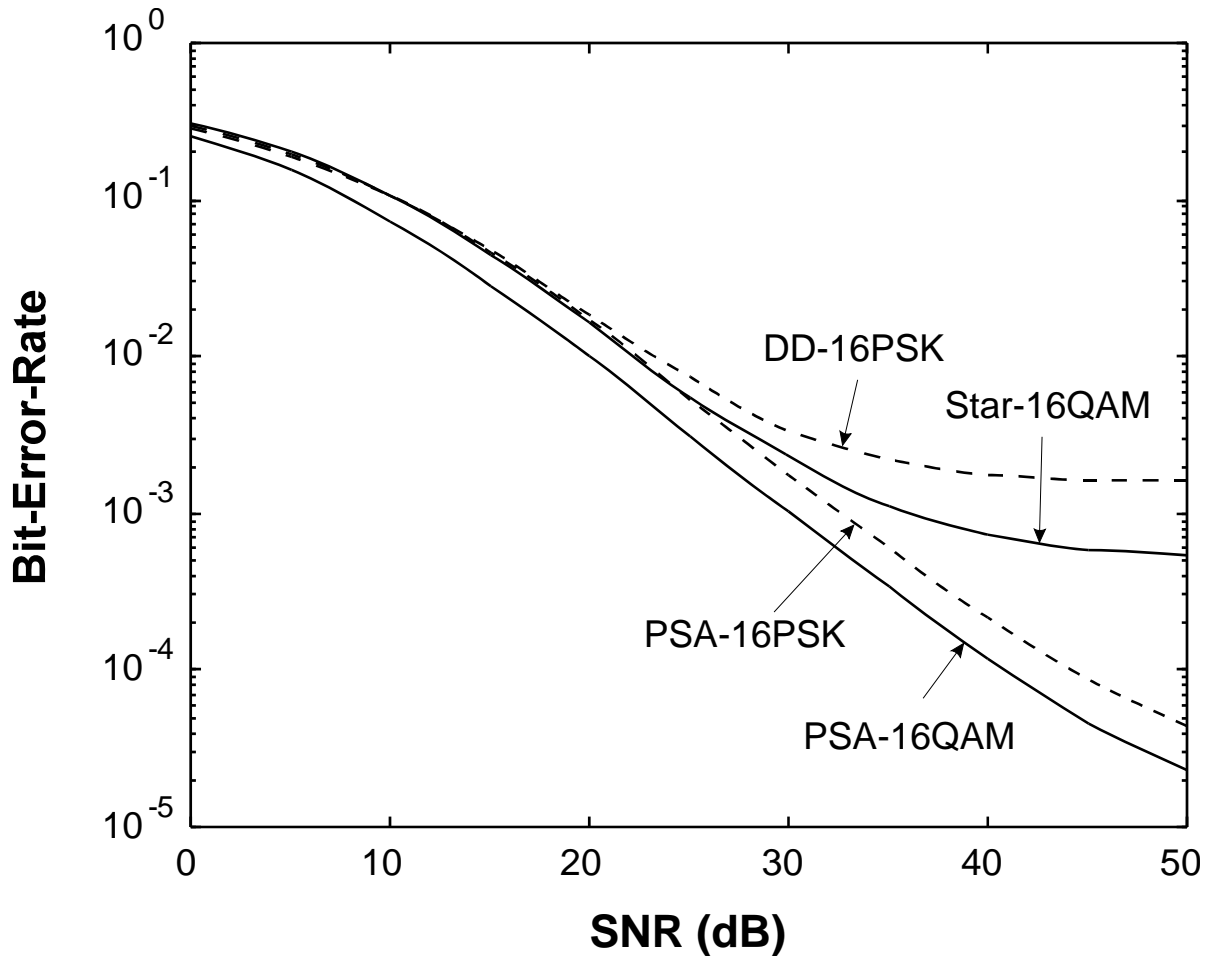**Fig. 5**   *Performances of 16PSK and 16QAM Signals in a Gaussian Channel*

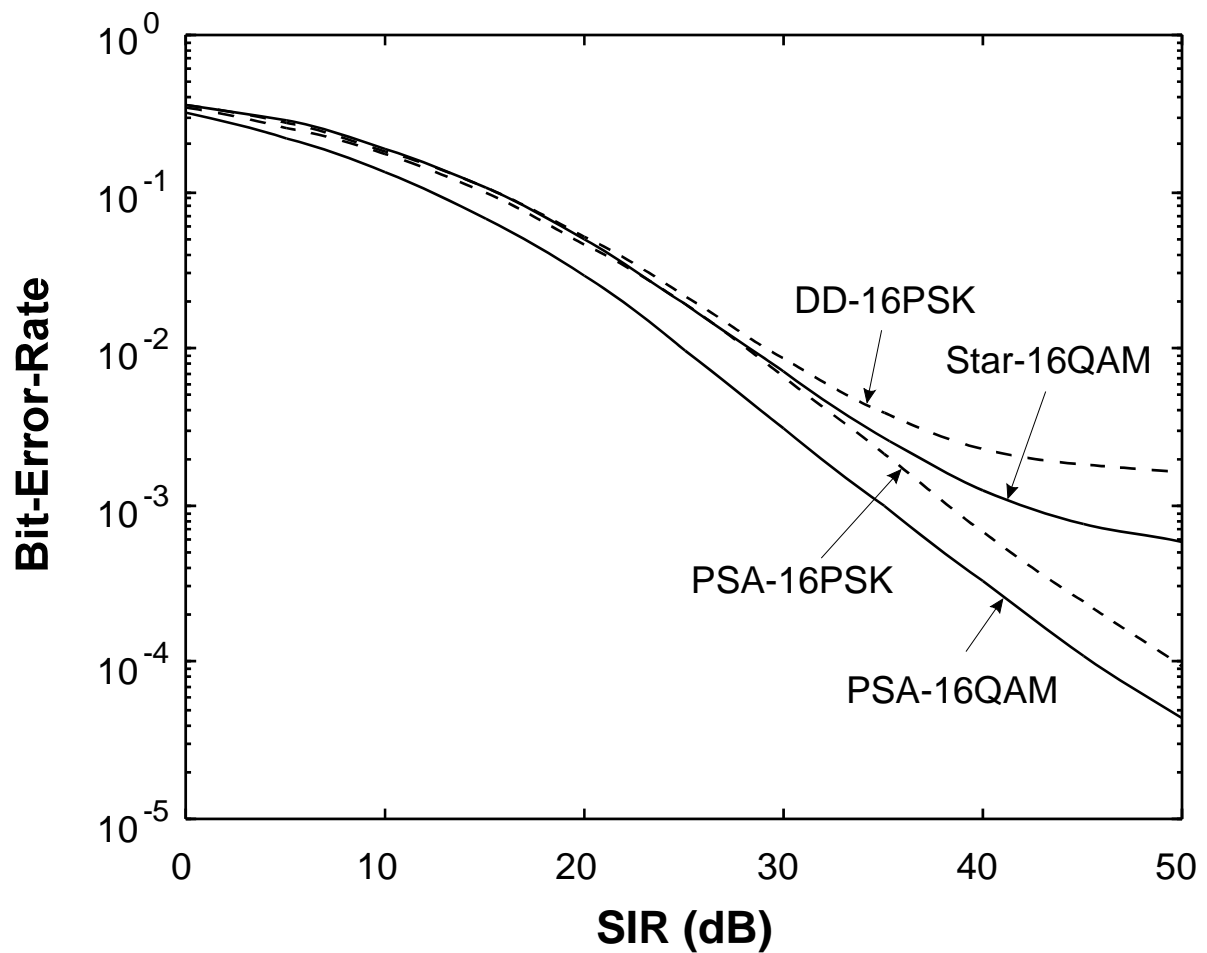**Fig. 6**   *BER Performances as Functions of SNR in the Frequency-Nonselective Channels and in the Absence of CCI*

Fig. 7   *BER Performances as Functions of SIR in the Frequency-Nonselective Channels and in the Absence of AWGN*
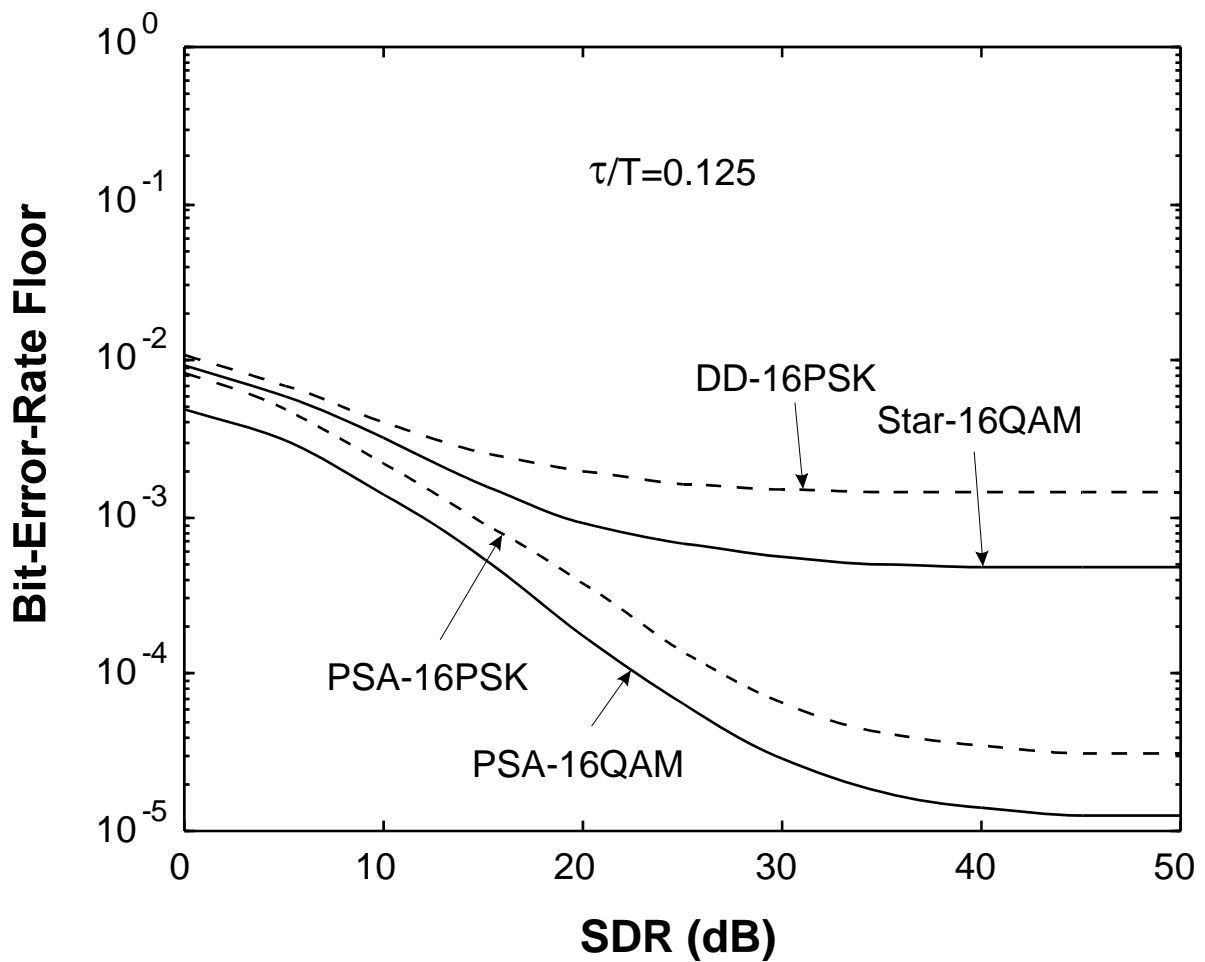
Fig. 8a   *BER Floors as Functions of SDR in the Frequency-Selective Channels with the Normalized Delay. (a)* $\tau / T = 0.125$.
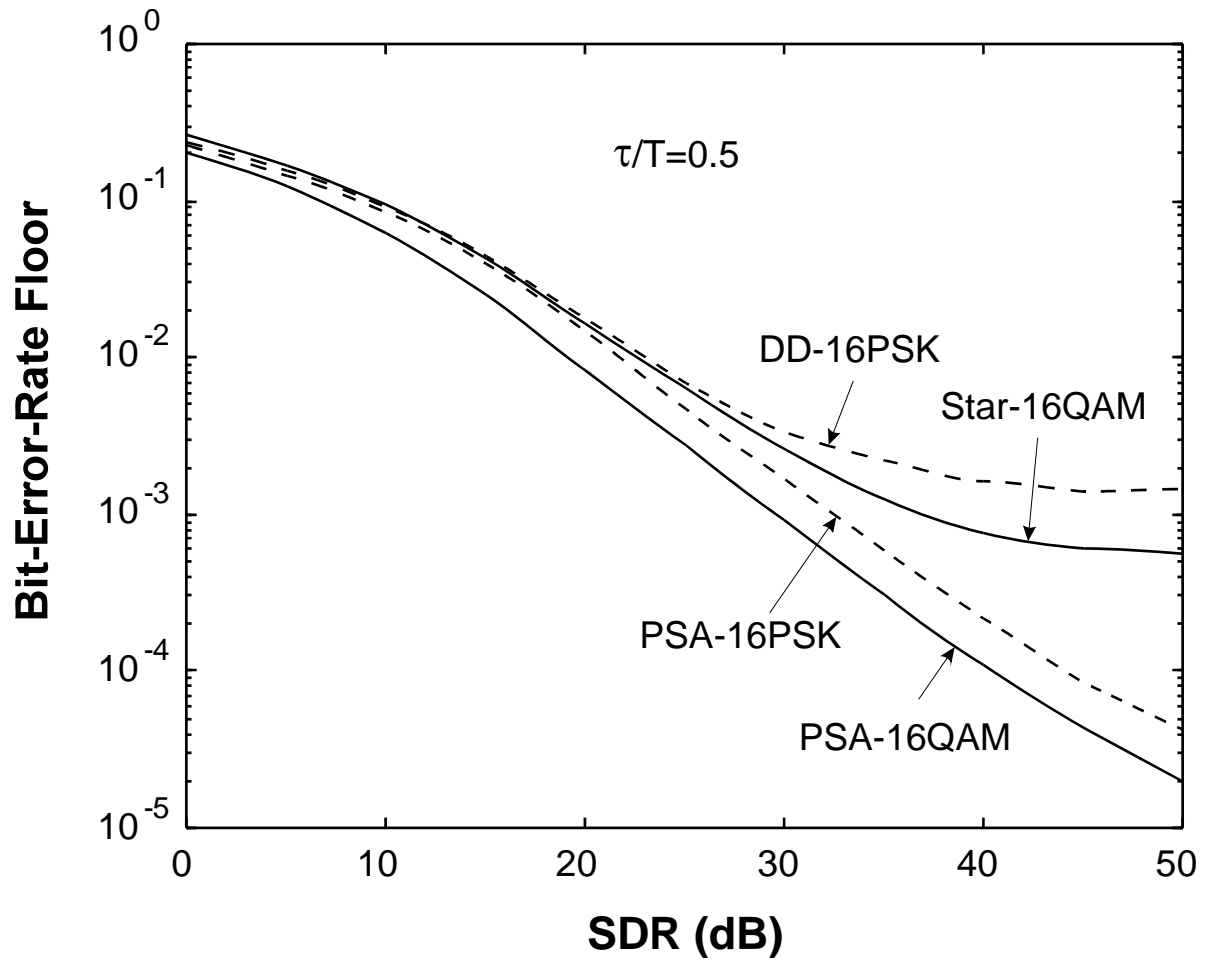
Fig. 8b   *BER Floors as Functions of SDR in the Frequency-Selective Channels with the Normalized Delay. (b) $\tau / T = 0.5$*
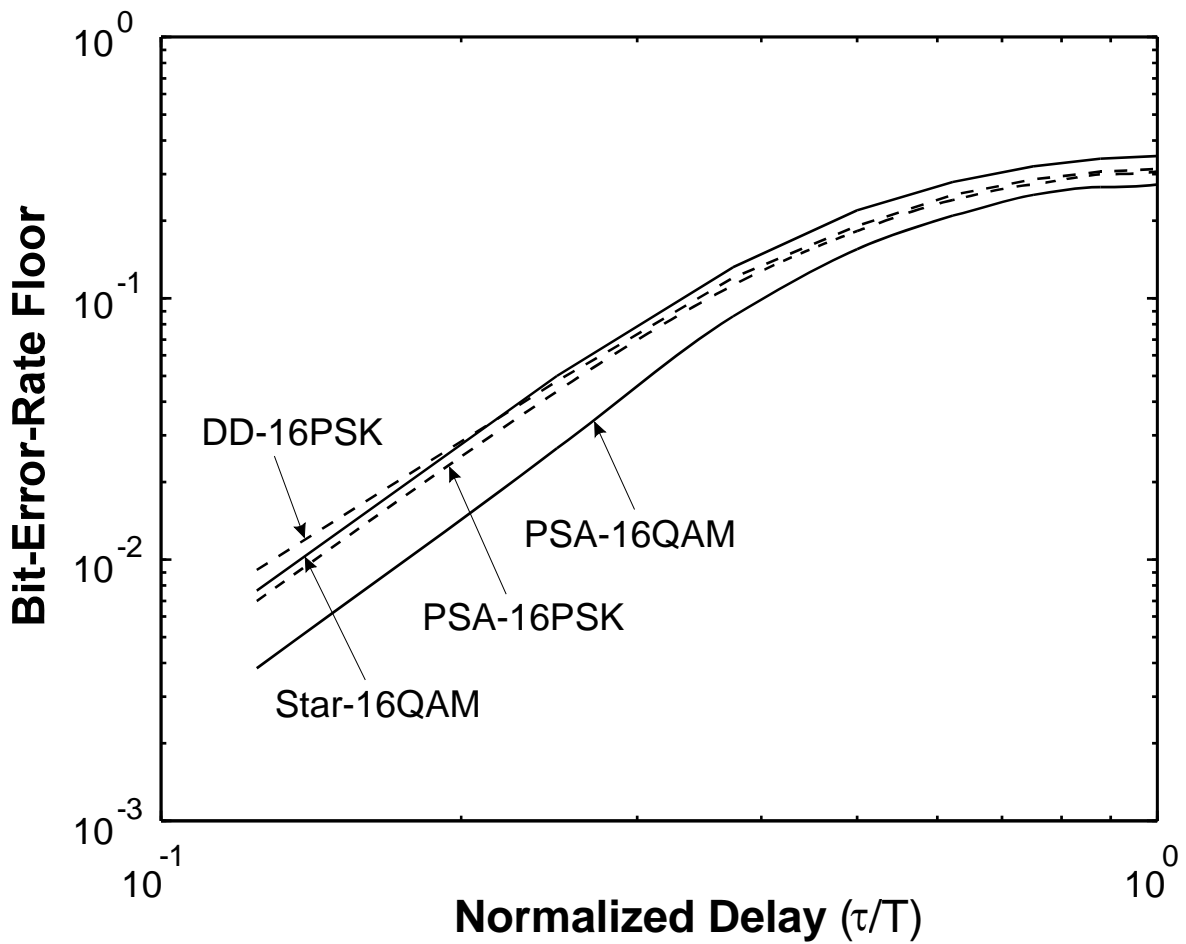
Fig. 9   *BER Floors as Functions of Normalized Delay τ / T in the Frequency-Selective Channels with $SDR = 3$ dB*